Journal of Arid Environments 129 (2016) 80–92

Contents lists available at ScienceDirect

Journal of Arid Environments

journal homepage: www.elsevier.com/locate/jaridenv

Monotemporal assessment of the population structure of *Acacia tortilis* (Forssk.) Hayne ssp. *raddiana* (Savi) Brenan in Bou Hedma National Park, Tunisia: A terrestrial and remote sensing approach

Frieke van Coillie [a, *], Kevin Delaplace [b], Donald Gabriels [c], Koen de Smet [d], Mohammed Ouessar [e], Azaiez Ouled Belgacem [e], Houcine Taamallah [e], Robert de Wulf [a]

[a] Ghent University, Laboratory of Forest Management and Spatial Information Techniques, Coupure Links 653, 9000 Gent, Belgium
[b] Intergraph Belgium, Tennessee House, Riverside Business Park, Bld International 55 E, 1070 Brussels, Belgium
[c] Ghent University, Department of Soil Management, Coupure Links 653, 9000 Gent, Belgium
[d] Flemish Government, Environment, Nature and Energy Department, Belgium, Koning Albert II-laan 20, bus 8, 1000 Brussel, Belgium
[e] Institut des Régions Arides de Médenine, 4119 Médenine, Tunisia

ARTICLE INFO

Article history:
Received 17 February 2014
Received in revised form
15 May 2015
Accepted 15 February 2016
Available online xxx

Keywords:
Remote sensing
Object-based image analysis

ABSTRACT

Soil erosion and desertification are the main problems faced by the Bou-Hedma National Park in South-Tunisia. Restoration of the original woodland cover, particularly by afforestation and reforestation with *Acacia tortilis* ssp. *raddiana*, has been recognized as efficient to combat further degradation of the environment in this protected area. In order to study effects of woodland restoration and future trends in Bou-Hedma, it is essential to accurately assess its current situation. This paper addresses a monotemporal assessment of the population structure of *A. tortilis*. An extensive field inventory was performed to provide deeper insight into the dendrometric characteristics of this keystone species. Next, a spatially explicit and repeatable method is developed to model key tree attributes like crown diameter, volume and tree height from which the structural composition of the *A. tortilis* population in the Bou Hedma National Park is derived. This method involves analysis of a very high resolution (VHR) GeoEye-1 image within an OBIA (Object-based Image Analysis) framework. The remote sensing (RS) results show that the population of *A. tortilis* is typified by an irregular population structure and confirm the findings of Noumi and Chaieb (2012) suggesting regressive population dynamics. The RS approach demonstrates potential for monitoring purposes in this particular setting of an arid environment.

1. Introduction

Acacia tortilis (Forssk.) subsp. *raddiana* (Savi) Brenan is one of the most important woody species in the pre-Saharan Tunisia zone. The species is able to tolerate extreme drought (in the range of 20–200 mm of annual rainfall) through special adaptations such as a deep lateral root system and partial shedding of leaves in the dry season. It is the only forest tree persisting on the edge of the desert (Abdallah et al., 2008; Grouzis and Le Floc'h, 2003; Noumi et al., 2010a, 2010b). In the past, as was the case for many other (semi-) arid zones, the Bou-Hedma National Park did not receive the necessary attention towards its biodiversity, protection and use. As a result, the Bou-Hedma region suffered from severe desertification caused by excessive livestock grazing, partial land clearance, plugging and subsequent effects such as soil erosion and massive loss of trees. In 1955 only a few old trees were left, while in 1853 this *Acacia* forest steppe was reported to cover more than 38.000 ha (Karem, 2001; Tarhouni, 2003). In the 1960s, the first actions were taken to combat erosion: 700 ha were fenced, a tree nursery was set up and three integral protection zones (IPZ) were established (Caron, 2001). Since 1970 these protective actions resulted in a gradual restoration of the vegetation (Tarhouni, 2003). In 1977, the park became part of the network of Biosphere Reserves of UNESCO. In 1985, regeneration actions were undertaken through tree planting. These paid off and in 2001, Caron (2001) reported that, as

* Corresponding author.
E-mail addresses: frieke.vancoillie@ugent.be (F. van Coillie), kevin.delaplace@intergraph.com (K. Delaplace), donald.gabriels@ugent.be (D. Gabriels), koen.desmet@lne.vlaanderen.be (K. de Smet), med.ouessar@ira.agrinet.tn (M. Ouessar), Azaiez.ouledbelgacem@ira.rnrt.tn (A.O. Belgacem), taamallah.houcine@ira.rnrt.tn (H. Taamallah), robert.dewulf@ugent.be (R. de Wulf).

http://dx.doi.org/10.1016/j.jaridenv.2016.02.009
0140-1963/

a result of these planting activities, the number of *A. tortilis* specimen increased with a factor of 30.

The restoration of the original forest steppe for the purpose of combating desertification, particularly by afforestation and reforestation, is therefore an important research item in the Bou-Hedma region. In a cooperation project between the Flemish Government of Belgium and the *Direction Générale des Forêts* of Tunisia, reforestation of 50,000 ha with *A. tortilis* is planned in the historical geographic range of the species (from Sidi Toui to the region of Tozeur) (Ouessar, 2011). Reforestation programmes like this one can contribute to worldwide environmental campaigns such as the Kyoto Clean Development Mechanism (CDM). These require scientific follow up of the plantations, including their ecological and socio-economical values (CDM-Home, 2010). Reforestation of *A. tortilis* is hypothesised to induce local climatic change in the Biosphere Reserve with consequences as 1) change of soil temperature, 2) improvement of soil fertility and nutrient status (Abdallah et al., 2008; Noumi et al., 2010a, 2010b), 3) improvement of the soil water availability (Noumi and Chaieb, 2012), 4) biodiversity increase (Abdallah et al., 2008), 5) influence on the cloud formation process inducing precipitation, and 6) interception of water by tree leaves and trunks mitigating erosion processes (Belgacem et al., 2013). The impact of this local climate change is already felt outside the Biosphere Reserve, where the local rural population depends on rain fed agriculture and water resources originating from water infiltrated on the mountains of the Bou-Hedma (Ouessar, 2011). Although the reforestation programs are evaluated positively, Noumi et al. (2010a) reported large-scale mortality and poor regeneration of *A. tortilis* trees within the National Park. Possible reasons for this disturbed level of natural regeneration include autoallelopathy (Noumi et al., 2010a) as well as high infestation rates by seed beetles like *Bruchidius raddianae* and *B. aurivillii* (Derbel et al., 2007). As yet the population of *A. tortilis* trees in Bou Hedma has been subject of several studies, particularly in the fields of phenology and ecophysiology (Schoenenberger, 1987). Recently Noumi and Chaieb (2012) systematically counted and measured all *A. tortilis* individuals, covering an area of 5114 ha. Although extremely useful as a reference database, this full inventory is highly labour intensive and yet remains a snapshot in time. We therefore investigated the potential of remote sensing image analysis to detect all *A. tortilis* trees that are spatially distributed around the National Park and to develop a practical, reliable and repeatable method to estimate their tree attributes. As drylands like the Bou-Hedma region are considered to have great potential for carbon sequestration (Lal, 2004a, 2004b, 2009), such a remote sensing tool could also serve to assess the magnitude of potential carbon sequestration, and hence could play an important role in regional climate change studies.

We first performed a field dendrometric study. The measured tree parameters served to establish empirical equations estimating individual *A. tortilis* tree attributes. Indirect tree attribute modeling was conducted based on object features derived from a Very High Resolution GeoEye-1 image. Next, the image classification results in conjunction with the empirical tree attribute equations served to assess the structure of the entire *A. tortilis* population in Bou-Hedma National Park. Finally, the modeled population structure was validated against the ground-based full inventory of Noumi and Chaieb (2012).

2. Materials and methods

2.1. Study area

Bou-Hedma National Park is situated in central Tunisia (34°24′N to 34°32′N and 09°29′E to 09°44′E) and is located along the southern Tunisian mountain ranges that are extensions of the Saharan atlas (Abdelkebir, 2005). The altitude varies between 90 m and 814 m above sea level (Abdelkebir, 2005). Bou-Hedma is characterized by an extremely irregular spatio-temporal rainfall pattern (Boukchina et al., 2006). The main climatic characteristics are an average annual rainfall of 180 mm, an average annual temperature of 17.2 °C, a mean maximum temperature of 38.0 °C and a mean minimum temperature of 3.9 °C. Following Demerger's classification the climate in Bou-Hedma National Park is Mediterranean arid with temperate winters (Noumi et al., 2010b) (Fig. 1).

The northern border of the National Park is mountainous. The mountain slopes are characterized by limestone bedrock (with some travertine deposits) which is exposed to severe water erosion, while the high mountain plateaus are typified by silty soils that are deep enough as rooting substrate (Karem et al., 1993). The foothills are marked by outcropping parent material, a limestone crust topsoil and accumulation of colluvial material. Water availability increases from the glacis (transition zone between mountain and plain) to the sandy plain because of increasing soil water holding capacity as well as increasing proximity of the water table (Noumi et al., 2010b). The *oueds* or *wadis*, dried temporal riverbeds, are very heterogeneous (sandy beds, rocks, pebbles) (Schoenenberger, 1987). The gypsum and salt alluvium plain southwards from the mountains consists of a deep coarse sandy soil with undeveloped deposits. These deposits date from the Quaternary and originate from the mountains. The heterogeneity in soil characteristics creates an edaphic environment (plant communities are distinguished by soil conditions rather than by climate conditions): psammophile species, such as *Rhanterium suaveolens* Desf. and *Cleome amblyocarpa* Baratte and Murb. depend on the sand/wind fixation phenomena on the calcareous gypsum crust (Schoenenberger, 1987).

The *A. tortilis* steppe is considered as a remainder of tropical origin (Sghari, 2009). Much of the Mediterranean basin became more arid in the period 1000–500 BC (Ouarda et al., 2009). However, it is generally agreed, that a more lush vegetation (capable of maintaining elephant populations), was present up to the second and third century of our era (Lavauden, 1928). Since the 3rd century, increasing aridity led to the gradual disappearance of tropical steppes at the northern border of the Sahara. This was also the case in Tunisia, which has lost its entire *Acacia raddiana* steppe, except for a reduced population that survived in Bou-Hedma. According to Sghari (2009), the survival of the steppe is a consequence of a geomorphologic shelter, created by the surrounding mountain ranges. In the North, there is the Djebel Bou-Hedma, which forms a barrier for the cold, moist wind from the northwest. This barrier also creates a totally different bioclimate at both sides of the Djebel Bou-Hedma. In the South, there is also a mountain range which protects the *A. tortilis* steppe from the warm, dry Saharan winds. Other theories claim that the highly polyploidy state (tetraploid) gives the population advantages in unstable environments, which is also observed with other species (e.g. *Atriplex halimus* L.) (Ouarda et al., 2009).

Belgacem et al. (2013) describe the vegetation of Bou-Hedma linked to the local morphology: the mountain massif is dominated by *Juniperus phoenacea* L., *Periploca angustifolia* Labill., *Rhus tripartitum* (Ucria) Grande, *Olea europea* L., *Rosmarinus officinalis* L. and *Stipa tenacissima* L. The piedmont is covered by *Artemisia herba-alba* Asso, *Anarrhinum brevifolium* Coss. & Kralik, *Gymnocarpos decander* Forssk. and *Helianthemum kahiricum* Delile. The subject species of this paper, *A. tortilis*, dominates the flat area as the only tree stratum.

Bou-Hedma National Park consists of 16,488 ha of *A. tortilis* forest steppe of which 8814 ha are managed under a system of integral protection. There are three Integral Protections Zones (IPZs) or core areas (resp. 5114 ha; 2660 ha and 1000 ha), two Buffer

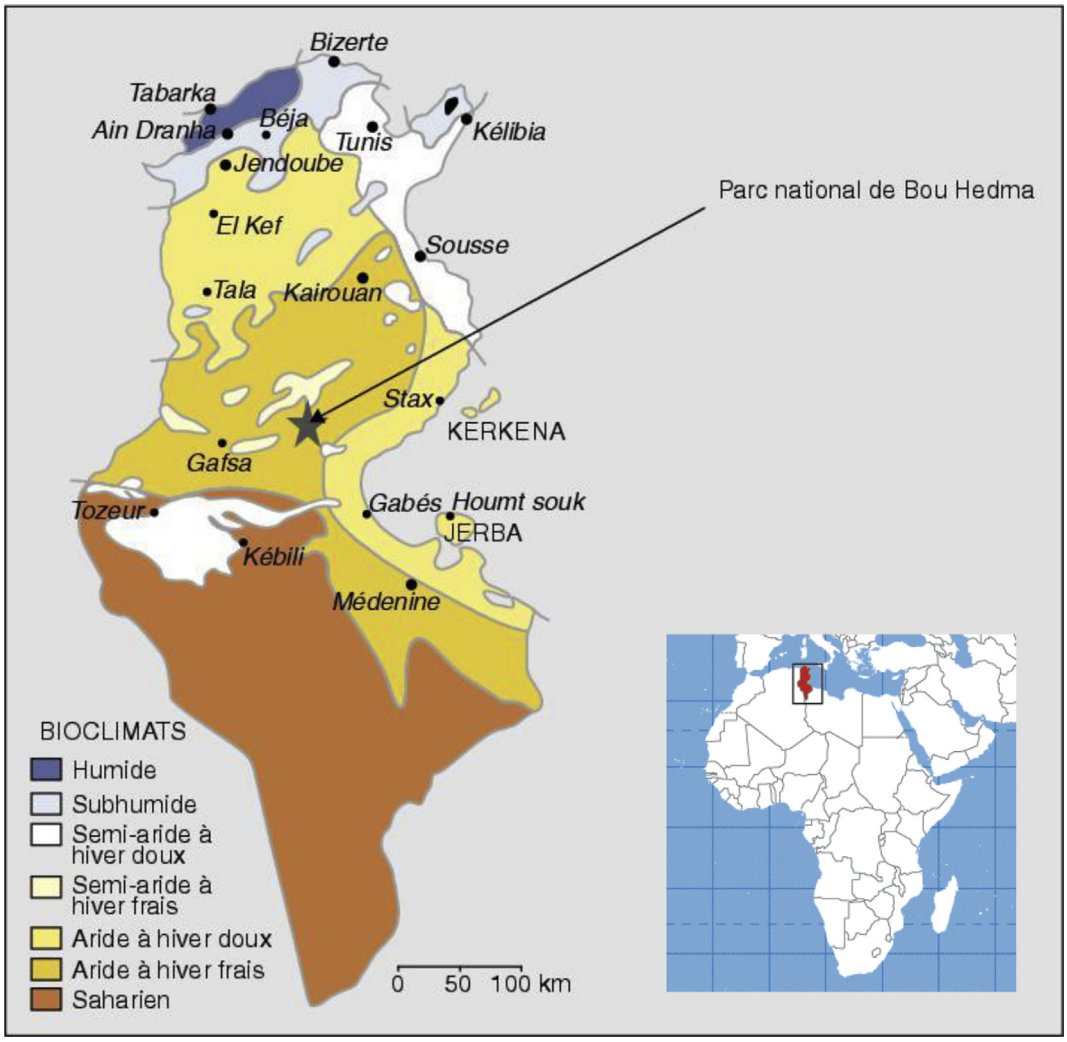

Fig. 1. Geographical location of Bou-Hedma National Park on the bioclimatic map of Tunisia (Tarhouni et al., 2007).

Zones (resp. 1774 ha and 2010 ha) and two Agricultural Zones or transition areas (resp. 2400 ha and 1500 ha). IPZ 1 is surrounded by a fence preventing wild animals (reintroduced *Addax* sp. and *Oryx* sp. antelopes, Mhorr gazelles, ostriches and mouflons) from escaping and avoiding grazing by domestic animals. Bou-Hedma Mountain is considered as a natural barrier, so no fencing is established at the north side. In this paper, we focus on IPZ 1 as study area (Fig. 2). In contrast to IPZ 1 neither the Agricultural nor Buffer Zones are fenced. All over the Agricultural Zones crop husbandry is scattered but has limited success due to unreliable yields. Only a part of the crops is irrigated, often by using water with a high salt content. *Tabias*, water harvesting structures used to limit sheet erosion and to increase water retention, are common practice (Ouessar, 2011). In the Buffer Zones all agricultural activities are prohibited, as is the harvesting of all natural resources (Caron, 2001).

2.2. VHR satellite data

The GeoEye-1 (formerly known as OrbView-5) satellite was launched on September 6, 2008. The Geo-Eye push broom imaging system records the reflected radiation from the Earth's surface in the blue (0.450–0.510 μm), green (0.510–0.580 μm), red (0.655–0.690 μm) and near-infrared (0.780–0.920 μm) portions of the electromagnetic spectrum with a spatial resolution of 2 m. A panchromatic band (0.450–0.800 μm) is also available with 0.41 m spatial resolution, which is resampled to 0.50 m for commercial customers. The radiometric resolution is 11 bits per pixel (GeoEye, 2009).

The optimal time of image acquisition is when possibilities to discriminate trees from soil and other vegetation are the highest. In this respect the dry season is considered as optimal, as no herbaceous vegetation is present increasing the contrast between trees and soil. Moreover, cloud cover then is generally very low. The acquired GeoEye-1 image (dating from 1st of August 2009 at 10:18 GMT), coincides with the period of maximum leaf development of *A. tortilis*. Cloud cover was 0%. The image was geometrically corrected (with a bias error of 1.66 m and a random error of 1.00 m) by GeoEye Inc. and provided in UTM (WGS 84) coordinates. Prior to analysis, the multispectral bands were pansharpened using the Graham Smith pansharpening algorithm (Laben and Brower, 2000) resulting in a spatial resolution of 0.5 m × 0.5 m per pixel.

2.3. Field data collection

All field measurements were performed in IPZ 1, the largest integral protection zone of the National Park. In Bou-Hedma, *A. tortilis* appears in two spatial configurations. First, scattered over

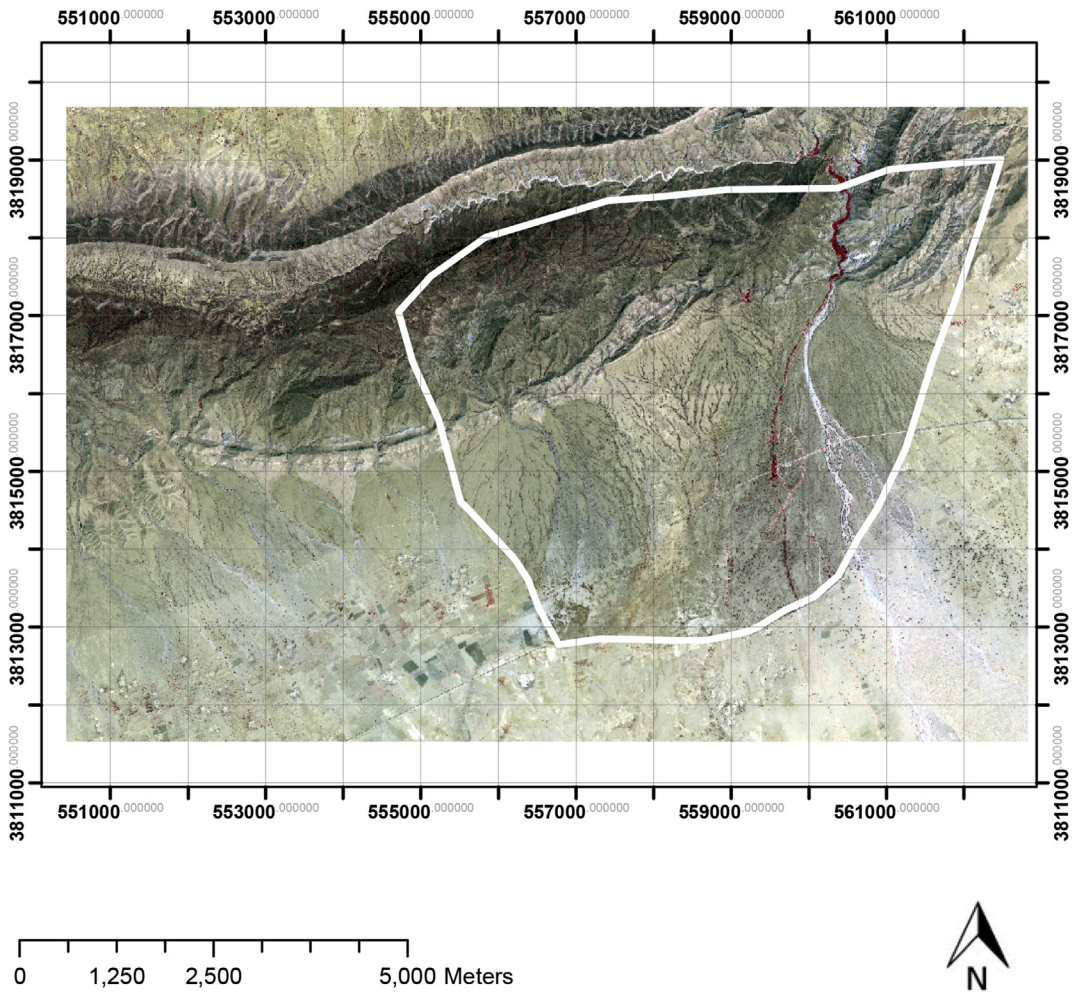

Fig. 2. Study area - Integral Protection Zone 1 (IPZ 1) (white polygon) located in the Bou-Hedma National Park (GeoEye-1 image, false colour composite, UTM (WGS 84)).

the entire National Park, linear formations of trees are found as relicts of former plantations. Secondly, *A. tortilis* trees also occur naturally in depressions and *oueds* where they grow with larger shrubs such as *Periploca* L. spp. and *Retama* Webb and Berthel spp.). Moreover, *Acacia* trees grow as solitaries as well as tree groups with touching crowns. Next to *Acacia* planted eucalypt trees are present, mainly located along the road (north-south orientation) and in some dense plantations close to the *Bordj* (military fortress or caravansary). Taking into account both spatial configurations (plantations versus 'natural') and tree appearances (individuals versus tree groups), 433 *A. tortilis* trees of different tree diameter classes were randomly sampled. Using a Garmin GPSMap 60Cx, tree coordinates were determined and stored in UTM units (WGS 84). Tree bole diameter (BOD) was measured at two reference heights (1.30 m and 0.10–0.15 m above the ground, resp. diameter at breast height (DBH) and basal diameter (BD)). Total tree height (TH) was measured with a clinometer (Suunto PM-5/360 S). Errors associated with height measurements were lower than 2% for objects on flat terrain. As slopes in IPZ 1 are gentle we expect measuring errors for trees on hilly terrain to remain in the range of 2%–5%, which is the average error reported by Needham and Peasly (2003). Finally, crown diameter (CD) was measured in two perpendicular directions (north-south and east-west direction). These directions were chosen in function of an additional objective (assessment of the influence of tree canopy on the herbaceous species composition and dry matter yields) that is not reported in the current paper. In case of tree groups, only the aggregate crown diameter was measured, because individual tree crowns were visually not distinguishable.

2.4. Dendrometric study

Field data were subjected to statistical analysis with the purpose of analysing the dendrometric characteristics of the *A. tortilis* trees. Appropriate tree attribute measures were calculated to compare results. For single-stemmed trees, these measures were maximum, resp. mean BD and DBH. For multi-stemmed trees, we computed the equivalent diameter, an adapted measure to estimate total multi-trunk woody plant diameter (Hoover, 2008; Noumi et al., 2010b) for both BD and DBH:

$$\textit{Equivalent Diameter} = \sqrt{\sum_{i}^{n} d_i^2} \quad (1)$$

with n = total number of stems
d_i = diameter of trunk i

In the absence of standardized tree volumes for the typical physiognomy of *A. tortilis*, we approximated bole volume by the

volume of a truncated cone:

$$Volume = \frac{\pi}{4} H \left(\frac{EqBD^2 + EqBD{*}EqDBH + EqDBH^2}{3} \right) \quad (2)$$

with $EqBD$ = equivalent basal diameter (m)
$EqDBH$ = equivalent diameter at breast height (m)
H = breast height (1.30 (m))

Prior to statistical analyses, parametric assumptions were checked. Normality was verified through QQ-plots and with the *Kolmogorov–Smirnov* (*K–S*) *Test for Normality* (H0: samples are normally distributed). Whenever normality tests yielded p-values < 0.05, it was ensured that more than 30 data points were in the dataset, allowing to perform the tests with lower power. Homoscedasticity was tested through the *Modified Levene Test* (H0: $\sigma_1^2 = \sigma_2^2 = \ldots = \sigma_n^2$). For all reported analyses, no data transformations were required to meet parametric assumptions for the statistical tests applied.

A Paired-Samples t-Test was performed to assess the directional variation in crown diameter, while a *Two-Sample t-Test* was used to analyse differences in tree attributes among individual trees and tree groups. One-way analysis of variance (ANOVA) was performed followed by Tukey's HSD test to analyse the differences in tree attributes among single-to multi-stemmed trees.

Finally, for individual *A. tortilis* trees, allometric relations were established to estimate two key tree attributes: total tree height and tree volume. Both attributes were modeled by crown diameter in order to serve as reference for the RS-based models. For model development training sets were assembled; for accuracy assessment independent test sets were used. The Root Mean Square Error (RMSE) and Mean Absolute Percentage Error (MAPE) served as accuracy assessment tools.

$$RMSE = \sqrt{\frac{\sum_{i=1}^{n} (f(x_i) - y_i)^2}{n}} \quad (3)$$

$$MAPE = \frac{1}{n} \sum_{i=1}^{n} \left| \frac{f(x_i) - y_i}{y_i} \right| \times 100 \quad (4)$$

with $f(x_i)$ = estimated value
y_i = actual value
n = number of test data points

2.5. Remote sensing image analysis

Given the very high resolution of the VHR GeoEye-1 image, *A. tortilis* tree crowns are represented by collections of adjacent pixels with similar values. Hence, Object-based Image Analysis (OBIA) was considered as an obvious approach for crown mapping. We designed an OBIA framework within eCognition Developer 8 (Definiens, 2009a, 2009b) that consisted of three analysis steps: 1) segmentation, 2) computation of a multi-dimensional object feature dataset, and 3) object classification. Next, crown diameter, tree height and volume were estimated based on object geometry features like Area, Length/Width, Ecliptic Fit, Border Index and Shape Index. Again, model accuracy was assessed on independent test objects via the accuracy measures RMSE and MAPE. Finally, we applied the regression models to estimate CD, BD and TH of all classified *A. tortilis* trees in the Bou-Hedma National Park. Tree volume was not estimated at the Park level as the accuracy of the volume regression model was judged too low to provide reliable volume information. The above regressions allowed us to set up distributions of crown diameter, bole diameter and tree height, as such describing the *A. tortilis* population structure.

3. Results

3.1. Dendrometric study

In approximately 10% (43 out of 433) of the sampled tree locations, an *A. tortilis* tree group was assessed.

3.1.1. Directional variation of crown diameter

For tree individuals as well as tree groups, the *Paired-Samples t-Test* yielded p-values of respectively 0.85 and 0.62. Hence, on the 5% significance level, there was no significant difference for both measuring directions. As a result, the arithmetic mean was used in subsequent analysis. (see Table 1).

3.1.2. Attribute comparison of tree individuals versus tree groups

Tree attribute summary statistics were calculated and are presented in Table 2.

The *Two-Sample t-Test* (*with unequal sample size*), comparing the different tree attributes for tree individuals and tree groups, indicated p-values lower than 0.05 for all tree attributes. Hence, statistical significant differences were assessed between the tree attributes of tree individuals versus tree groups.

3.1.3. Attribute comparison of single-versus multi-stemmed trees

Attribute comparison was performed for tree individuals (390 out of 433 sampled locations). Almost 50% (193 out of 390 trees) of the sampled trees featured a single stem. Less than 10% of the individuals had more than 4 stems (Fig. 3). Based on this distribution, we considered 4 stem categories: 1 stem, 2 stems, 3 stems and ≥4 stems, ensuring the presence of more than 30 samples within each category.

Summary statistics were calculated generally indicating higher tree attribute means for single-versus multi-stemmed trees (Table 3). For all tree attributes, one-way ANOVA, comparing means of two or more stem categories, yielded p-values < 0.05. Hence, at the 5% level of significance, tree attributes differed significantly for at least two stem categories. A clear difference between single- (category 1) and multi-stemmed trees (categories 2, 3 & 4) was found for the attributes TH, maximum BD and, mean and maximum DBH: single-stemmed trees featured larger attribute values than multi-stemmed individuals. Regarding CD, no significant difference was found between single- and 4-stemmed trees, indicating that 4 or more stems significantly increased crown diameters. Compared to multi-stemmed trees, single-stemmed individuals featured significantly larger mean BD. Moreover trees with 2 stems showed a significantly larger mean BD than 3-stemmed trees, while for maximum BD no significant differences were found between these categories. Equivalent BD showed again other results: category 3 & 4 appeared significantly different. For DBH, a clear discrimination between single- and multi-stemmed trees exists. For equivalent DBH, category 4 significantly differed from categories 2 & 3, which was expected considering the higher equivalent BD for this category. As to volume, statistical differences were found between single-stemmed trees and trees with 2 or 3 stems. Volume differences between trees with one stem and 4 or more stems were not significant. Generally, the summary statistics showed lower attribute values for trees with 2 or 3 stems in comparison with single stemmed trees, but this was not the case for trees with more than 3 stems.

Table 1
Summary statistics of crown diameter in two perpendicular directions based on 433 samples (390 tree individuals, 43 tree groups).

Statistic	CD in N–S direction (m)	CD in E–W direction (m)	Mean CD (m)
Tree individuals			
Mean	4.85	4.91	4.88
Standard Deviation	2.60	2.62	2.59
Minimum	0.50	0.54	0.52
Maximum	14.60	14.75	14.25
Tree groups			
Mean	9.85	10.31	10.08
Standard Deviation	5.01	3.56	3.91
Minimum	3.40	2.70	3.05
Maximum	32.75	17.40	24.93

Table 2
Summary statistics of tree attributes based on 433 samples (390 tree individuals, 43 tree groups).

Tree attributes	Mean	Standard deviation	Minimum	Maximum
Tree individuals				
CD (m)	4.88	2.58	0.52	14.25
TH (m)	3.61	1.63	0.43	11.74
Mean BD (cm)	19.1	15.2	1.1	120.0
Maximum BD (cm)	21.4	15.2	1.6	120.0
Equivalent BD (cm)	23.5	15.6	2.0	120.0
Mean DBH (cm)	7.7	6.6	1.4	54.0
Maximum DBH (cm)	13.0	9.1	1.5	54.0
Equivalent DBH (cm)	21.8	13.8	2.1	67.0
Tree groups				
CD (m)	10.08	3.91	3.05	24.93
TH (m)	5.19	1.46	1.90	8.82
Mean BD (cm)	21.8	11.0	5.4	47.2
Maximum BD (cm)	36.1	15.0	10.3	70.1
Equivalent BD (cm)	52.3	20.9	14.6	126.5
Mean DBH (cm)	9.4	5.1	2.1	28.6
Maximum DBH (cm)	20.7	10.2	2.5	47.6
Equivalent DBH (cm)	44.8	20.7	4.1	120.3

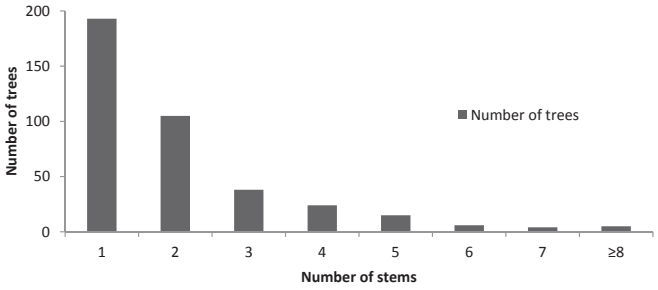

Fig. 3. Frequency distribution of number of stems for 390 *Acacia* tree individuals.

3.1.4. Attribute modeling: estimating tree height and tree volume from field-measured CD

Tree height and tree volume are two attributes that are often estimated via allometric modeling based on bole diameter (BOD). This approach avoids a large amount of tedious measurements. In this study relationships are built with CD instead of BOD. For many tree species stable linear relationships have been described between CD and BOD. An example of such an approach for open grown trees in Kenya has been described by Mugo et al. (2011). This approach is obvious in view of the developed remote sensing (RS) procedure where TH and V are estimated via RS geometry features that are strongly related with CD. The use of CD instead of BOD is corroborated by the high linear correlations that were assessed between CD and all BOD measures. Correlations between CD and mean BD, maximum BD and equivalent BD were respectively 0.81, 0.88 and 0.92. Linear correlations between CD and mean DBH, maximum DBH and equivalent DBH were respectively 0.82, 0.90 and 0.94.

Allometric relations (least squares fit) were established between both tree height and tree volume, and CD. A 3/4 power law relation (Fig. 4) was found between crown diameter and total tree height featuring a R^2 of 0.86, RMSE of 0.770 m and MAPE of 15.7%.

$$TH\ (m) = 1.1332 \times CD\ (m)^{0.7439} \quad (5)$$

A strong allometric relation likewise existed between the estimated tree volume from base to 1.30 m, and crown diameter. This model featured a R^2 of 0.93, with a RMSE and MAPE of respectively 45.989 dm^3 and 31.7%.

$$Volume\left(dm^3\right) = 0.8319 \times CD\ (m)^{2.503} \quad (6)$$

3.2. Remote sensing image analysis

3.2.1. Image segmentation

Homogeneous image segments (or objects) were derived from the input scene through image segmentation. Two different algorithms were sequentially applied. First a *multi-resolution* segmentation (bottom-up algorithm) was executed followed by a *contrast split* segmentation (top-down approach) (Benz et al., 2004). For both segmentations, the algorithms' parameters were determined by trial and error on a subset of the image containing both *A. tortilis* and eucalypt trees. Parameter values for *multi-resolution* segmentation were set to 0.2 for shape and 0.5 for compactness respectively. These settings prioritized colour over shape. The initial *multi-resolution* segmentation resulted in image objects correctly representing larger trees. However, smaller trees were often wrongly outlined and mainly included in larger segments with multiple smaller trees and soil/vegetation cover in between. Therefore, sequential *contrast split* segmentation was performed, largely isolating smaller trees (Fig. 6). The split was based on the contrast present in the pansharpened NIR band. Although the majority of trees were successfully delineated, conscientious inspection revealed that there were still a few isolated segmentation errors for trees with CDs smaller than 3.5 m.

3.2.2. Computation of multi-dimensional object feature dataset

A. tortilis trees were separated from other trees, soil and shrub segments by classification based on a variety of object features. Three land cover classes were considered: *A. tortilis*, Eucalyptus and Bare soil (the latter including shrubs like *Periploca* sp., *Retama* sp. and *Hammada* sp.). A total of 470 object features grouped into 68 categories (Table 4) were synthesized providing an informative characterization of the image objects in terms of spectral

Table 3
Summary statistics of tree attributes for each of the four stem categories. Superscripts indicate the non-significantly different categories as defined by the Tukey method.

Number of stems category	Sample size	Mean	Standard deviation	Minimum	Maximum
CD (m)					
1	193	5.6^{ac}	2.64	0.79	14.25
2	105	3.94^{b}	2.21	0.84	12.45
3	38	3.79^{b}	2.27	0.52	9.10
≥4	54	4.86^{c}	2.49	1.16	11.10
TH (m)					
1	193	4.18^{a}	1.69	0.63	11.74
2	105	3.02^{b}	1.35	0.56	10.25
3	38	2.82^{b}	1.51	0.43	7.62
≥4	54	3.26^{b}	1.29	0.82	7.14
Mean BD (cm)					
1	193	27.5^{a}	16.5	2.1	120.0
2	105	12.1^{b}	8.0	1.5	44.1
3	38	9.2^{c}	7.1	1.1	28.1
≥4	54	9.3^{bc}	5.9	1.3	27.0
Maximum BD (cm)					
1	193	27.5^{a}	16.5	2.1	120.0
2	105	15.7^{b}	11.6	2.0	72.2
3	38	13.1^{b}	9.9	1.6	43.1
≥4	54	16.7^{b}	10.9	2.1	43.8
Equivalent BD (cm)					
1	–	–	–	–	–
2	105	18.2^{ab}	12.5	2.2	73.3
3	38	17.1^{a}	12.9	2.0	53.0
≥4	54	23.8^{bc}	15.1	2.8	62.2
Mean DBH (cm)					
1	193	9.6^{a}	7.8	1.6	54.0
2	105	5.8^{b}	4.5	1.4	30.9
3	38	5.0^{b}	2.8	1.5	10.7
≥4	54	5.7^{b}	3.0	1.4	13.5
Maximum DBH (cm)					
1	193	15.1^{a}	10.2	2.1	54.0
2	105	9.5^{b}	7.2	1.5	44.4
3	38	9.2^{b}	5.7	2.2	19.8
≥4	54	10.7^{b}	5.8	1.6	24.0
Equivalent DBH (cm)					
1	–	–	–	–	–
2	105	16.8^{ab}	11.6	2.1	60.5
3	38	17.5^{ab}	11.8	4.3	50.3
≥4	54	22.2^{b}	13.0	2.7	54.6
Volume (dm^3)					
1	193	94.8^{a}	109.1	1.2	891.5
2	105	49.0^{bc}	71.4	2.2	459.0
3	38	51.4^{bc}	61.0	3.6	272.3
≥4	54	79.2^{ac}	81.9	2.4	336.9

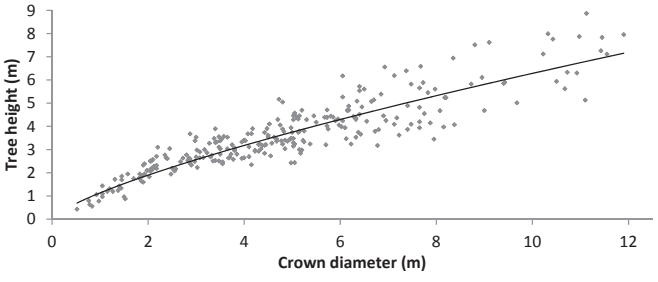

Fig. 4. TH (m) in function of CD (m), based on measurements on 390 *Acacia* specimen.

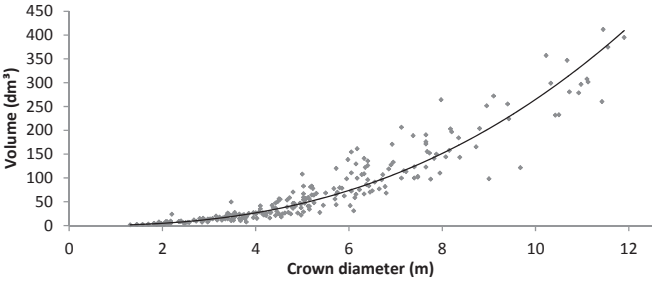

Fig. 5. Volume (dm^3) in function of CD (m), based on measurements on 390 *Acacia* specimen.

reflectance, geometry and texture.

3.2.3. Object classification

Through Feature Space Optimization (FSO), the combination of object features which were most suitable to discriminate between different land cover classes was assessed. The FSO algorithm compares the object features searching for feature combinations that produce the largest average minimum distance between class samples. Based on an image subset, FSO yielded an optimal feature set of 34 object features (out of 20 categories (Table 4)). Next, object statistics of this optimized feature space were calculated and used to classify all image objects (500,000 segments) based on their nearest sample neighbours (nearest neighbour classification). Fig. 7 shows the classification result for a subset of the image scene. The three land cover classes are rendered in colour with *A. tortilis* in green, Eucalyptus in red, and Bare Soil in olive. The remaining non-classified image objects are buildings and roads. An accuracy

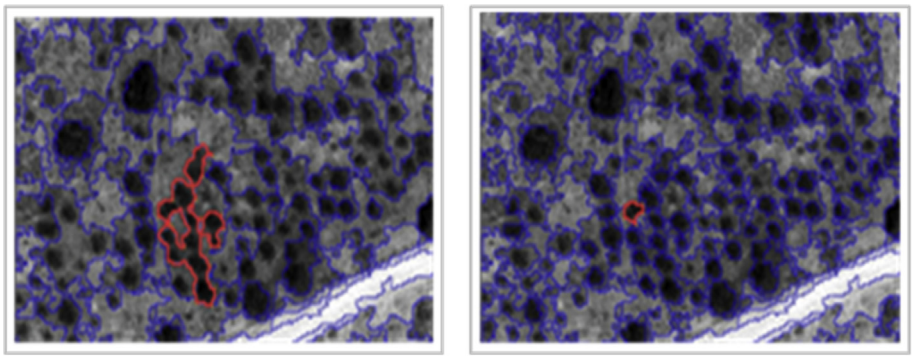

Fig. 6. Results of the initial *multi-resolution* segmentation (left) and subsequent *contrast split* segmentation (right) overlayed on the pansharpened NIR band.

Table 4
Feature categories used for object characterization with in bold the categories applied for classification.

Type	Feature
Customized	**FDI** [a], **NDVI**, **SAVI**
Layer Values	**Border contrast**, Brightness, **Circular mean**, Circular StDev, Circular StDev/Mean, **Contrast to neighbour pixels**, **Edge contrast of neighbour pixels**, Max difference, **Max**, Mean difference to brighter neighbours, Mean difference to neighbours, Mean of inner border, **Mean of outer border**, **Mean**, **Min**, Skewness, **StDev to neighbour pixels**, StDev
Geometry	Area, **Asymmetry**, Average area represented by segments, Average branch length, Average length of edges, Border index, Border length, **Compactness**, Curvature/length, Degree of skeleton branching, **Density**, Elliptic fit, Length of longest edge, Length of main line, Length, Length/Thickness, Length/Width, Length/Width, Main direction, Maximum branch length, Number of edges, Number of inner objects, Number of pixels, Number of segments, Perimeter, Polygon self-intersection, Radius of largest enclosed ellipse, Radius of smallest enclosing ellipse, Rectangular fit, Relative border to image border, Roundness, Shape index, StDev Curvature, StDev of area represented by segments StDev of length of edges, Thickness, Volume, Width
Texture after Haralick et al. (1973)	**Angular 2**nd **moment**, Contrast, **Correlation**, Dissimilarity, **Entropy**, **Homogeneity**, **Mean**, StDev

[a] The Forest Discrimination Index (FDI) (Bunting and Lucas, 2006) was adjusted for the GeoEye-1 image (FDI=NIR-(R−B)).

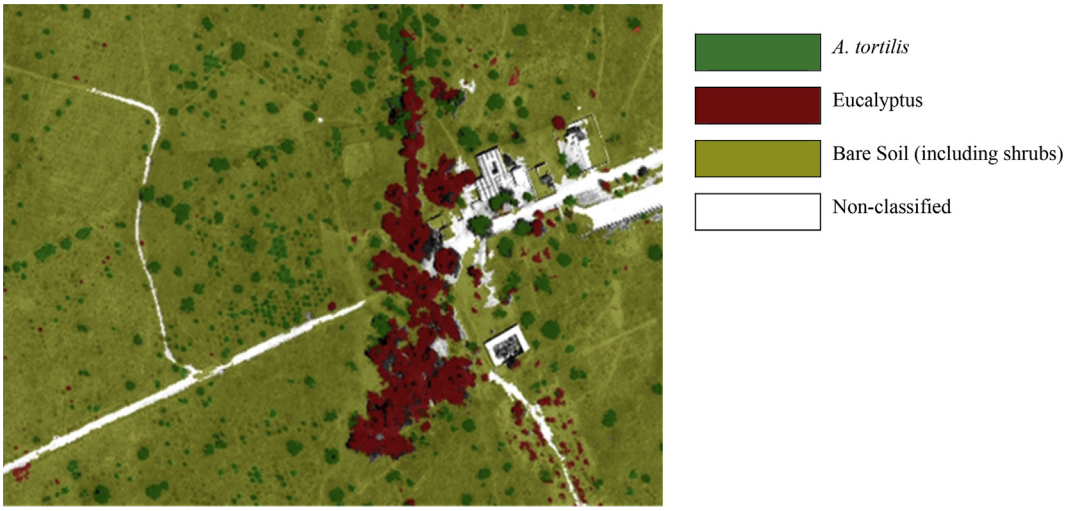

Fig. 7. Subset of the object-based classification result.

assessment was performed on a limited number of test samples (roughly 5000 segments) yielding a high, but somewhat biased (all *A. tortilis* segments were used as test samples) Kappa Index of Agreement of 0.95.

3.2.4. Attribute modeling: estimating tree height and tree volume from RS-derived CD

Based on the object features, Decision Tree Analysis (Chubey et al., 2006) was implemented to distinguish between tree individuals and tree groups. With only 19 out of 43 tree groups successfully identified, the method failed to adequately separate tree groups from tree individuals. Therefore, before modeling, large *A. tortilis* segments (tree groups) were eliminated. Besides, small *A. tortilis* segments were also dropped because of the observed segmentation errors for trees with CD < 3.5 m, leaving 344 tree individuals in the dataset: 139 to build the models, 205 to test their accuracy (randomly selected).

The dendrometric study above showed that TH and V could reliably be estimated via CD field measurements (Figs. 4 and 5). First, we tested whether CD could be estimated from RS images via

object geometry features related to crown dimensions. Next, we used the modeled CD to estimate TH and V. Appropriate object geometry features were *Area* (i.e. the number of pixels forming an image object), *Length/Width* (i.e. the ratio of the eigenvalues of the covariance matrix (raw image data), with the larger eigenvalue being the numerator of the fraction), *Ecliptic Fit* (describing how well an image object fits into an ellipse of similar size and proportions with 0 indicating no fit, and 1 indicating a perfect fit), *Border Index* (describing how jagged an image object is and calculated as the ratio between the border lengths of an image object and the smallest enclosing rectangle), and finally *Shape Index* (describing the smoothness of an image object and calculated from the object's border length divided by four times the square root of its area). In order to account for object shape, we constructed ratios between *Area* and the other geometry features. Regression models were fitted through the training data points, resulting in five models estimating CD (Table 5).

From the R^2, RSME and MAPE values, the best model to predict CD was the one based on the Area/LW ratio. This model showed a R^2 of 0.74, a RMSE of 1.108 m and MAPE of 15.8% (Fig. 8).

$$CD\ (m) = 1.6223 \times Area/LW\ \left(m^2\right)^{0.4169} \quad (7)$$

Next, the models for total tree height and tree volume were likewise selected. The model estimating total tree height using the Area/LW ratio showed a R^2 of 0.71, RMSE of 0.692 m and MAPE of 13.5%. The relation between Area/LW and tree height showed a 1/3 power trend (Fig. 9).

$$TH\ (m) = 1.5723 \times Area/LW\ \left(m^2\right)^{0.3116} \quad (8)$$

The relation between the estimated tree volume and the Area/LW ratio showed a power trend with a R^2 of 0.72, with a RMSE and MAPE of respectively 44.433 dm^3 and 51.9%. Considerable variance however was noticed, especially in the high values range (Fig. 10).

$$Volume\ \left(dm^3\right) = 2.3671 \times Area/LW\left(m^2\right)^{1.1008} \quad (9)$$

While both TH and V were reasonably estimated based on RS-measured CD via the Area/LW ratio, the models based on field-measured CD featured higher R^2 values. However, accuracy and precision in terms of RMSE and MAPE of the RS models were higher with the exception of MAPE on V.

3.2.5. Assessment of forest structure, height and density

In our study, structure is defined as the arrangement of both crown and bole diameters. Likewise to CD, we first modeled mean BD based on Area/LW ($R^2 = 0.59$, RMSE = 0.90 m, MAPE = 15.1%). Next, the regression models were applied to estimate CD, mean BD and TH of all classified *Acacia* trees in the Bou-Hedma National Park.

3.2.5.1. Structure. The distribution of crown diameters derived from the GeoEye-1 image shows a clear dominance of CD classes 3–4 m and 4–5 m (Fig. 11 (left)). An exponential decrease is perceptible for tree crown diameters of 5 m and more. Small-sized crown diameter classes are characterized by lower frequencies with juvenile classes (CD < 2 m) merely counting 509 individuals (i.e. 2.3% of the total modeled population). Fig. 11 (right) illustrates the distribution of mean BD classes. BD shows roughly the same distribution as CD with marginal presence of juvenile individuals, dominance of trees with basal diameters between 10 and 15 cm and exponential decrease of larger-sized trees with mean BDs from 15 cm and more.

Table 5
Regression models based on the geometry features Area, Area/(Length/Width (LW)), Area/Ecliptic Fit (EF), Area/Border Index (BI) and Area/Shape Index (SI).

	CD	R^2	RMSE (m)	MAPE (%)
Area	$y = 1.4008x^{0.4381}$	0.7375	1.263	16.4
Area/LW	$\mathbf{y = 1.6223x^{0.4169}}$	0.7404	1.108	15.8
Area/EF	$y = 1.3463x^{0.4086}$	0.6735	1.238	19.2
Area/BI	$y = 1.4785x^{0.458}$	0.7218	1.153	15.6
Area/SI	$y = 1.5615x^{0.45}$	0.7269	1.150	16.1

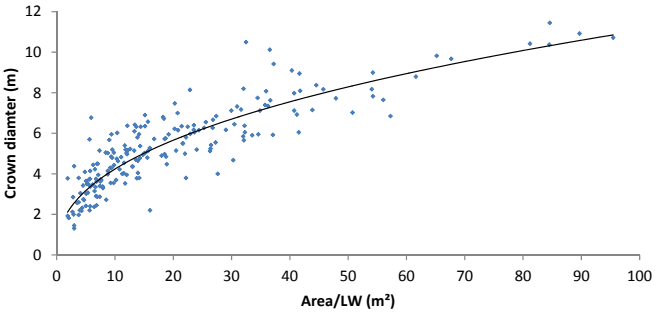

Fig. 8. CD (m) in function of Area/LW ratio (m^2).

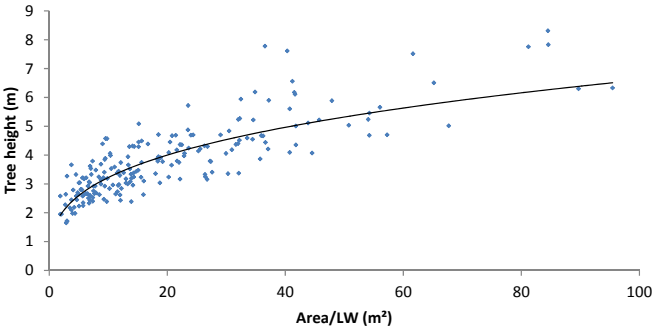

Fig. 9. TH (m) in function of Area/LW (m^2).

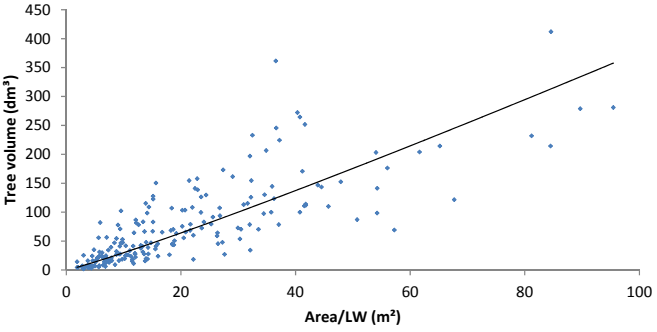

Fig. 10. Volume (dm^3) in function of Area/LW (m^2).

3.2.5.2. Height. Tree height classes between]2,3] m and]3,4] m are most prominent and together include 15,282 trees which is 69.7% of the total modeled population. Likewise, young and small trees occur rather rarely in comparison with older specimen with again an exponential decrease of trees higher than 4 m (Fig. 12).

3.2.5.3. Density. Density, i.e. number of trees per hectare, was

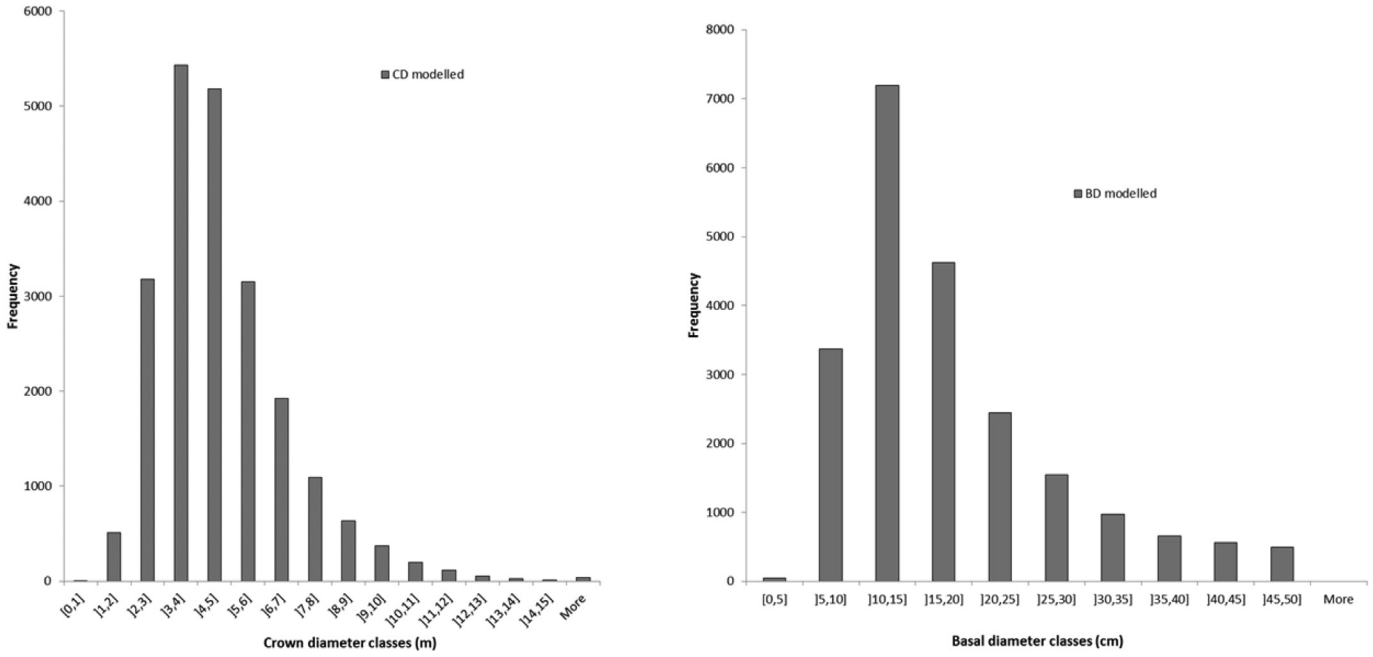

Fig. 11. Modeled CD (left) and mean BD (right) distribution.

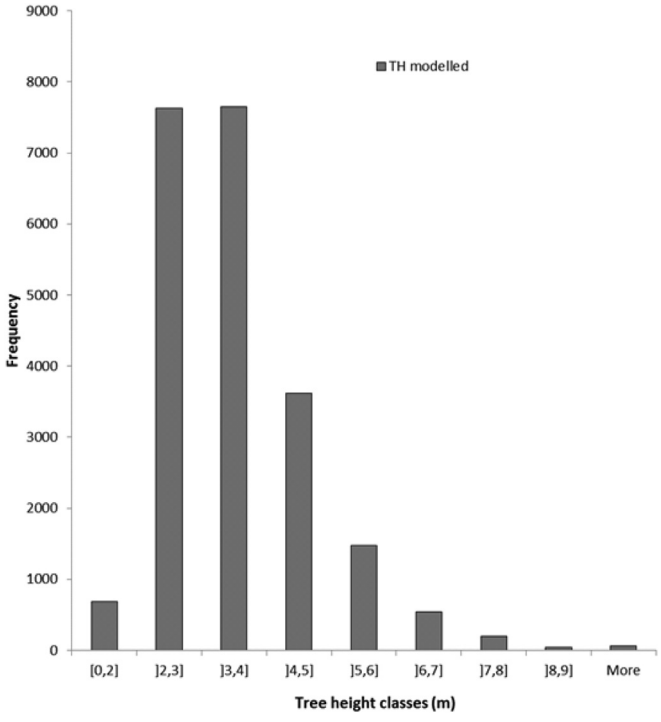

Fig. 12. Modeled TH distribution.

determined by using non-overlapping kernels of 1 ha (200 × 200 pixels, 0.5 m resolution). In order to exclude border effects kernels remained 100 pixels (50 m) away from the park boundary. In 760 of the 1 ha plots, no trees were present. We found a mean density of 8.4 trees per ha for the IPZ 1 of the Bou-Hedma National Park, with a median value of 5.0 trees per ha. A maximum density of 95 trees per hectare was determined in dense plantations close to the Bordj.

4. Discussion

4.1. Dendrometric study

From the dendrometric study, based on 433 sampled trees, it was concluded that 90% of the *A. tortilis* trees appeared as tree individuals. Only 10% were tree groups with intersecting crowns. Neither for the tree individuals nor for the tree groups, directional variation in crown diameter was assessed. Compared to tree groups, tree individuals showed significantly lower attribute values relating to CD, BD, DBH and TH. Larger CDs for tree groups were logical as total crown diameter was measured. Larger equivalent BD/DHB was evident as these measures aggregated all stems. In semi-arid regions, light conditions generally have no strong impact on tree architecture (Archibald and Bond, 2003). Nevertheless, larger tree heights were found for tree groups compared to tree individuals. Knowing that, for a tree group, TH was determined by the highest tree in the group, this indicated possible interaction between trees in a group. DBH (as well as equivalent DBH/BD) was significantly higher for tree groups, which was not expected as trees subjected to light competition generally feature smaller bole diameters. However, the tree groups in our dataset are probably old relicts of the ancient forest which may clarify the larger bole diameters. Unfortunately, no data are available to validate this assumption and thus to discriminate between planted trees and natural relicts. Finally, both for tree individuals and groups, CD was larger than TH (Mihidjay, 1999) confirming that *A. tortilis* trees in this arid environment generally grow wide (Archibald and Bond, 2003).

From the comparison between single versus multi-stemmed trees, we learned that approximately half of the sampled tree individuals featured a single stem, while the other half was multi-stemmed with less than 10% having more than 4 stems (Fig. 3). In the field *A. tortilis* thus displayed a variable physiognomy with many trees featuring a bushy appearance. According to Mihidjay (1999), the bushy aspect is typical for young individuals which are multi-stemmed from the base. At a certain age (starting from approximately 10 years), one of the axes becomes the trunk while

others are inhibited. According to Mihidjay (1999), the inhibited axes degenerate afterwards. Sometimes the bifurcation at the base remains (2–3 branches), however these individuals seem more retarded in their growth (Mihidjay, 1999). Based on our results the hypotheses of Mihidjay (1999) could not be rejected, or accepted. In Bou-Hedma National Park, both young and aged trees with multiple stems occurred. Generally, single stemmed trees showed larger attribute values than trees with 2 or 3 stems; however, this was not always true for trees with more than 3 stems. This raises the question whether multiple stems should be considered as a characteristic of the species. The results of the dendrometric study provided a comprehensive overview of the properties of the sampled *A. tortilis* population in Bou-Hedma National Park. Unfortunately, due to lack of reference information, it was not possible to confirm that tree groups were old relicts of ancient forests and that a multi-stemmed appearance might be a morphological characteristic of *A. tortilis*.

Finally, the allometric equations allowed to determine TH and V based on field-measured CD with relatively high accuracy levels. However, given the increasing variance with increasing CDs, the model results for tree individuals with CD > 5 m should be considered less reliable.

4.2. Remote sensing image analysis

The developed OBIA approach allowed to detect and classify most *A. tortilis* trees occurring in the National Park. During the classification process 21,910 segments were classified as *A. tortilis*. As tree groups were included, these segments did not necessarily represent individual trees. According to Noumi and Chaieb (2012) there are approximately 23,191 tree individuals in IPZ 1 of the Bou-Hedma National Park. The underestimation of trees is caused by the fact we managed to only partly split tree groups into tree individuals combined with the slightly less successful segmentation of smaller tree crowns. Moreover, based on the multi-dimensional feature dataset no reliable distinction could be made between individuals and tree groups (decision tree analysis). For modeling purposes, we therefore eliminated tree groups from the dataset. As a result, the assessment of the structure of the *A. tortilis* population was biased. Under the present conditions the employed strategy is valid as groups were only a limited fraction of the total population (approximately 10% based on random sampling). Moreover, as tree groups have larger crown diameters this was prominent mainly in larger CD classes. This bias was noticeable when comparing the RS-measured CDs and mean BDs against the field-measured diameters (Fig. 13). The RS method systematically underestimated both juvenile and large-sized individuals while adult trees with CDs between 3 and 5 m were overestimated. Apart from that, both CD and BD distributions were fairly similar.

From their full inventory, Noumi and Chaieb (2012) concluded that, out of 23,191 *A. tortilis* trees, respectively 12% and 18% had a trunk circumference (measured at ground level) between 20 and 30 cm, and 30 and 40 cm (Fig. 14). These percentages were also predicted using the RS models (after transforming diameters to circumferences). Again, both juvenile and large-sized classes were systematically under- and overestimated by the RS models. Apart from these modeling errors, the population structure of *A. tortilis* showed the same trend as assessed by Noumi and Chaieb (2012): dominance of adult trees with high circumferences and marginal presence of juvenile individuals suggesting a low regeneration rate.

The results of the density analysis were also in line with the labour-intensive tree counting performed by Noumi and Chaieb (2012). They found about 5 individuals or less per hectare; the RS procedure yielded a median density value of 5.0 trees per ha in IPZ 1, with a maximum density of 95 trees per ha in dense plantations close to the Bordj.

As the RS analysis mainly confirmed the foundings of Noumi and Chaieb (2012) describing regressive dynamics of the *A. tortilis* population in Bou Hedma, we consider RS as a valuable technique to assess population structure. The strength of the RS method is its spatially explicit character and its automatic and repeatable usability. In order for the RS method to be eligible as a reliable monitoring tool assessing population dynamics, the segmentation procedure must be improved for both small and large tree individuals. One avenue to explore is to exchange the multi-resolution/contrast-split segmentation approach by a centre-weighed segmentation method. Earlier research suggested that segmentation algorithms based on homogeneity are often not succesful for tree crown delineation (Tiede et al., 2006). Centre-weighed algorithms that are based on local maxima detection of assumed tree tops might offer more potential and should be tested on their capacity to delineate both small and large *A. tortilis* trees more accurately. A disadvantage of centre-weighed algorithms might be the fact that these are often region-specific, i.e. a priori knowledge of the scale domain of the envisaged target object is needed. In other words, the approximate crown diameter of both small and large trees must be known in advance, as this knowledge serves to coordinate object growth and to implement the algorithm's stopping criteria.

5. Conclusions

Since the 3rd century AD increasing aridity led to the gradual disappearance of tropical steppes at the northern border of the Sahara. This was likewise the case in Tunisia that lost its entire *A. tortilis* forest steppe, except for a reduced population that survived in Bou-Hedma. To date desertification is still combated mainly by restoration of the original woodland particularly by means of reforestation and afforestation. As these restoration measures are assumed to induce local climate changes, knowledge of the number of trees and their attributes is an essential part in understanding their impact. Based upon the recent developments in VHR RS for forest inventory and assessment, we developed a framework that incorporates VHR satellite images into an object-based tree attribute estimation process rendering valuable information on crown diameter, bole diameter, tree height and volume distributions over the entire National Park. The framework integrates elements of automated image segmentation, feature-based classification and indirect attribute modeling finally assessing the structure, height and density of the *A. tortilis* forest steppe in Bou-Hedma National Park. With RMSE values of resp. 1.108 m, 0.90 m, and 0.692 m, the established models were found to adequately estimate crown diameter, mean basal diameter and tree height. Although comparable to volume estimations based on field measurements, due to considerable variance for large-sized trees, we recommend careful interpretation of the RS-based volume predictions. Finally, based on the classification results the RS-based models were spatially deployed thereby registering the current structural status of the *A. tortilis* forest steppe in Bou-Hedma National Park. In essence, the results confirmed the conclusions of Noumi and Chaieb (2012) that the population of *A. tortilis* in the region of Bou Hedma is characterised by an irregular structure, whereby regressive dynamics of the species is assumed. In order to claim the presented framework to be robust further fine-tuning is necessary: small trees should be missed less and tree groups should be split better. Possible remediation points in the direction of centre-weighed segmentation. Although open to improvement, the presented framework can easily be adapted to other VHR image types and different ecosystem attributes providing forest managers and policy makers with basic information for planning purposes.

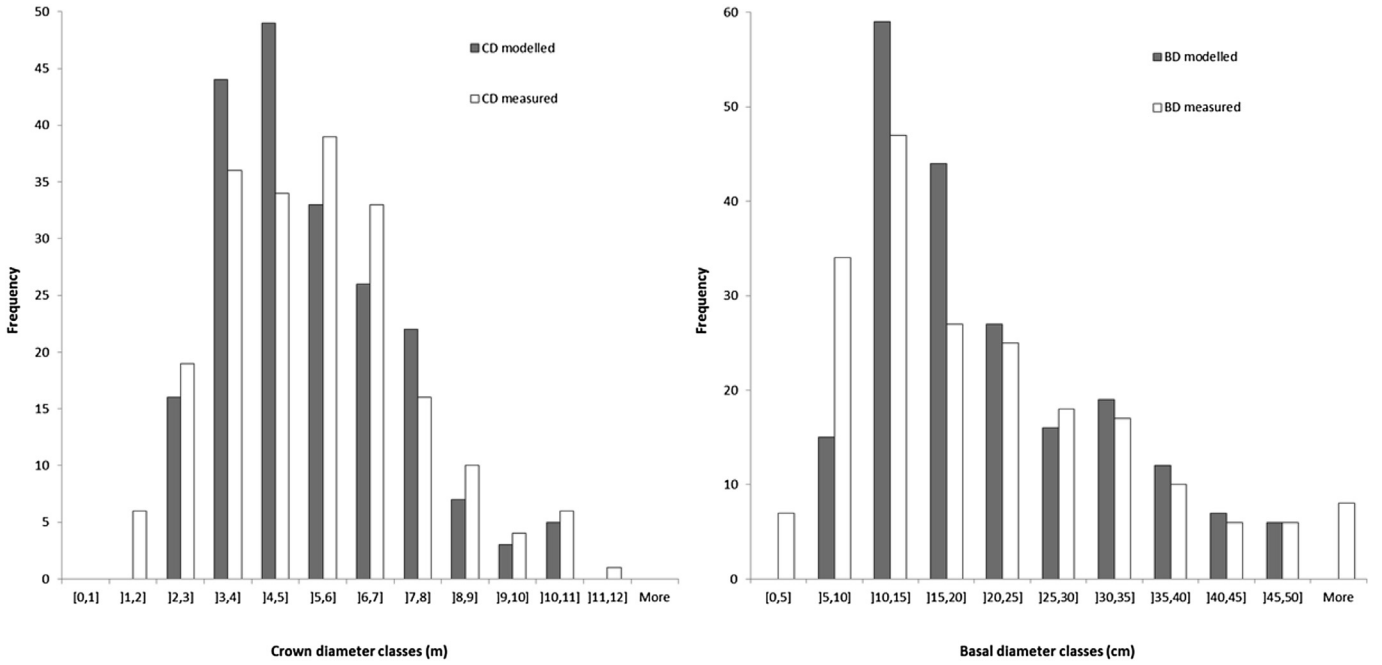

Fig. 13. Modeled against measured CD and mean BD distribution.

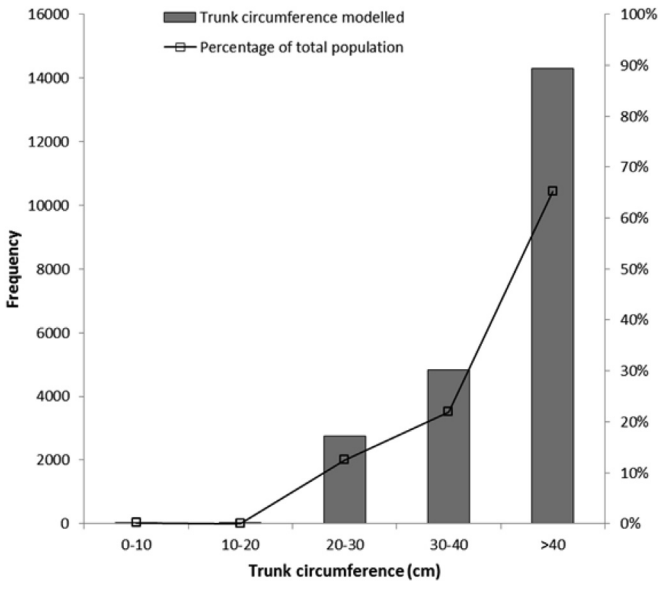

Fig. 14. Modeled trunk circumference distribution (size classes according to Noumi and Chaieb (2012)).

Acknowledgments

The authors thank the Flemish Government for providing the GeoEye-1 imagery. Special thanks go to ir. Lazhar Hemdi, head of the Bou-Hedma National Park, for his enthusiasm and collaboration during the field work. The anonymous reviewers are thanked for their constructive remarks and suggestions.

References

Abdallah, F., Noumi, Z., Touzard, B., Belgacem, A.O., Neffati, M., Chaieb, M., 2008. The influence of *Acacia tortilis* (Forssk.) subsp. *raddiana* (Savi) and livestock grazing on grass species composition, yield and soil nutrients in and environments of South Tunisia. Flora 203, 116–125.

Abdelkebir, H., 2005. Elaboration de la carte des aménagements CES et de lutte contre l'ensablement dans l'observatoire de Haddej Bou Hedma par la technique de SIG. Thesis. Université de Jendouba, Ecole Supérieure des Ingénieurs de l'Equipement Rural de Medjez-El-Bab, p. 83.

Archibald, S., Bond, W.J., 2003. Growing tall vs growing wide: tree architecture and allometry of Acacia karroo in forest, savanna, and arid environments. Oikos 102, 3–14.

Belgacem, A.O., Tarhouni, M., Louhaichi, M., 2013. Effect of protection on plant community dynamics in the mediterranean arid zone of southern Tunisia: a case study from bou hedma national park. Land Degrad. Dev. 24 (1), 57–62.

Benz, U.C., Hofmann, P., Willhauck, G., Lingenfelder, I., Heynen, M., 2004. Multi-resolution, object-oriented fuzzy analysis of remote sensing data for GIS-ready information. ISPRS J. Photogramm. Remote Sens. 58, 239–258.

Boukchina, R., Ouled Belgacem, A., Taamallah, H., Ouessar, M., Dhaoui, M., Selmi, S., 2006. Surveillance biophysique dans l'observatoire de Haddej Bou Hedma – Tunisie. Institut des Régions Arides, Médenine, Tunisia, p. 145.

Bunting, P., Lucas, R., 2006. The delineation of tree crowns in Australian mixed species forests using hyperspectral Compact Airborne Spectrographic Imager (CASI) data. Remote Sens. Environ. 101, 230–248.

Caron, S., 2001. Suivi écologique de l'Oryx algazelle (*Oryx dammah*) dans le parc National de Bou-Hedma (Tunisie) et notes sur les autres Ongulés sahélo-Sahariens du parc. Travail de fin d'étude en vue de l'obtention du grade académique de Diplôme d'Etudes Supérieures Specialisées. Université des Sciences et technologies de Lille, France.

CDM-Home, 2010. http://cdm.unfccc.int/index.html (accessed 22.09.10).

Chubey, M.S., Franklin, S.E., Wulder, M.A., 2006. Photogramm. Eng. Remote Sens. 72 (4), 383–394.

Definiens, 2009a. eCognition Developer 8. User Guide. Definiens AG, München, Germany.

Definiens, 2009b. eCognition Developer 8. Reference Book. Definiens AG, München, Germany.

Derbel, S., Noumi, Z., Anton, K.W., Chaieb, M., 2007. Life cycle of the coleopter *Bruchidius raddianae* and the seed predation of the *Acacia tortilis* subsp. *raddiana* in Tunisia. *Comptes Rendus Biol.* 330, 49–54.

GeoEye, 2009. GeoEye-1 Fact Sheet. http://launch.geoeye.com/LaunchSite/about/fact_sheet.aspx (accessed 20.09.10).

Grouzis, M., Le Floc'h, E., 2003. Un arbre au désert, Acacia raddiana. IRD Editions, Paris.

Haralick, R.M., Shanmuga, K., Dinstein, I., 1973. Textural features for image classification. IEEE Trans. Syst. Man Cybern. 610–621. SMC3.

Hoover, C.M., 2008. Field Measurements for Forest Carbon Monitoring. A Landscape-Scale Approach. Springer Science + Business Media B.V, New York.

Karem, A., Ksantini, M., Schoenenberger, A., Waibel, T., 1993. Contribution à la régénération de la végétation dans les Parcs Nationaux en Tunisie aride. Eschborn: GTZ.

Karem, A., 2001. Le rôle des parcs nationaux et les réserves naturelles dans la conservation de la biodiversité. Rev. Des. Régions Arid. 2001, 293–302.

Laben, C.A., Brower, B.V., 2000. Process for Enhancing the Spatial Resolution of

Multispectral Imagery Using Pansharpening. US Patent 6 011 875.
Lal, R., 2004a. Carbon sequestration in dryland ecosystems. Environ. Manag. 33 (4), 528–544.
Lal, R., 2004b. Soil carbon sequestration impacts on global climate change and food security. Science 304, 1623–1627.
Lal, R., 2009. Sequestering carbon in soils of arid ecosystems. Land Degrad. Dev. 20, 441–454.
Lavauden, L., 1928. La forêt de gommiers du bled talha (Sud-tunisien). Revue des Eaux Forêts 66, 699–713.
Mihidjay, A.S., 1999. Etude de la morphogenèse d'Acacia tortilis (Forsk.) Hayne ssp. raddiana (Savi) Brenan et essais de regeneration in vitro. Memoire de diploma d'études approfondies en physiologie vegetale. Université de Tunis II, Tunisia.
Mugo, J., Njunge, J., Malimbwi, R., Kigomo, B., Mwasi, B., Muchiri, M., 2011. Models for predicting stem diameter from crown diameter of open grown trees in Sondj-Nyando river catchment, Kenya. Asian J. Agric. Sci. 3 (2), 119–126.
Needham, T., Peasley, N., 2003. The ASDM Stand Interventions Encyclopedia. The Forestry Resource Book of the Future – Today. http://www.unb.ca/standint/ (accessed 8.04.10).
Noumi, Z., Chaieb, M., 2012. Dynamics of *Acacia tortilis* (Forssk.) Hayne subsp *raddiana* (Savi) Brenan in arid zones of Tunisia. Acta Bot. Gallica 159, 121–126.
Noumi, Z., Ouled Dhaou, S., Abdallah, F., Touzard, B., Chaieb, M., 2010a. Acacia tortilis subsp. raddiana in the North African arid zone: the obstacles to natural regeneration. Acta Bot. Gallica 157, 231–240.
Noumi, Z., Touzard, B., Michalet, R., Chaieb, M., 2010b. The effects of browsing on the structure of *Acacia tortilis* (Forssk) Hayne subsp. *raddiana* (Savi) Brenan along a gradient of water availability in arid zones of Tunisia. J. Arid Environ. 74, 625–631.
Ouarda, H.E., Walker, D.J., Khouja, M.L., Correal, E., 2009. Diversity analysis of *Acacia tortilis* (Forsk.) Hayne ssp *raddiana* (Savi) Brenan (Mimosaceae) using phenotypic traits, chromosome counting and DNA content approaches. Genet. Resour. Crop Evol. 56, 1001–1010.
Ouessar, M., 2011. Drylands Management in the Arid Regions of Tunisia. Watershed of Zeuss-Koutine and Bou Hedma Biosphere Reserve (Tunisia). Progress Report of SUMAMAD Activities. http://www.unesco.org/new/fileadmin/MULTIMEDIA/HQ/SC/pdf/pub_sumamad_tunisia_national_report_9th_international_workshop_proceeding.pdf (consulted 02.12.13).
Schoenenberger, A., 1987. Rapport phytoécologique sur le Parc National de Bou Hedma. Projet GTZ N° 82.2045, p. 42.
Sghari, A., 2009. À propos de la présence d'une steppe tropicale au Jebel BouHedma en Tunisie présaharienne: approche géomorphologique. Quaternaire 20, 255–264.
Tarhouni, M., 2003. Cartographie des systèmes écologique et étude de la dynamique de l'occupation des terres dans le parc national de Bou Hedma. Thesis. Université de Sfax pour le Sud, Faculté des Sciences de Sfax, p. 94.
Tarhouni, M., Ouled Belgacem, A., Neffati, M., Chaieb, M., 2007. Dynamique des groupements végétaux dans une aire protégée de Tunisie mériodinale. Cah. Agric. 16 (1), 7.
Tiede, D., Lang, S., Hoffmann, P., 2006. Domain-specific class modelling for one-level representation of single trees. In: Blaschke, T., Lang, S., Hay, G. (Eds.), Object-based Image Analysis: Spatial Concepts for Knowledge-driven Remote Sensing Applications, pp. 237–256. ISBN: 978-3-540-77057-2, p133-151.

List of Abbreviations

A. tortilis: Acacia tortilis ssp. raddiana
BD: Basal Diameter
BOD: Bole Diameter
CD: Crown Diameter
CDM: Kyoto Clean Development Mechanism
DBH: Diameter at Breast Height
Eq: Equivalent
FSO: Feature Space Optimization
OBIA: Object-Based Image Analysis
GLCM: Grey Level Co-occurrence matrix
IPZ: Integral Protection Zone
MAPE: Mean Absolute Percentage Error
MS: Multi-spectral
NIR: Near Infrared
PAN: Panchromatic
RMSE: Root Mean Square Error
StDev: Standard Deviation
TH: Tree Height
VHR: Very High Spatial Resolution